Chemical Science

RSC Publishing

EDGE ARTICLE

View Article Online
View Journal | View Issue

Cite this: *Chem. Sci.*, 2013, **4**, 2471

Electrical conductance study on 1,3-butadiyne-linked dinuclear ruthenium(II) complexes within single molecule break junctions†

Hui-Min Wen,‡[a] Yang Yang,‡[b] Xiao-Shun Zhou,[c] Jun-Yang Liu,[b] Dao-Bin Zhang,[a] Zhao-Bin Chen,[b] Jin-Yun Wang,[a] Zhong-Ning Chen*[a] and Zhong-Qun Tian*[b]

Received 2nd February 2013
Accepted 18th March 2013

DOI: 10.1039/c3sc50312g

www.rsc.org/chemicalscience

Single-molecule conductance of three sulphur-functionalized organometallic wires with two ruthenium(II) centres spaced by 1,3-butadiyne was firstly investigated using an electrochemically assisted-mechanically controllable break junction (EC-MCBJ) approach. It is demonstrated that single-molecular conductance of these diruthenium(II) incorporated systems is significantly higher than oligo(phenylene-ethynylene) (OPE) having comparable lengths and exhibits weaker length dependence. The conductance improvement in these diruthenium(II) molecules is ascribable to the better energy match of the Fermi level of gold electrodes with the HOMO that is mainly resident on the Ru–C≡C–C≡C–Ru backbone. Furthermore, modulation of molecular conductance is achieved by changing the length and π-conjugated system of the chelating 2,2′:6′,2″-terpyridyl ligand.

Introduction

Single-molecule electronics has attracted great interest because its potential as a complement to silicon-based electronics in terms of a bottom-up approach and ultimate miniaturization.[1,2] Nevertheless, the realization of active molecular devices is highly challenging and is still far from maturity to date. The development of molecular electronics is mainly dependent on the improvement of molecular junction characterization methods[3] as well as design and synthesis of specific block molecules.[4,5]

Concerning molecular junction characterization, several techniques such as STM-break junction, crossing wires and mechanically controllable break junction (MCBJ) *etc.* have been implemented to measure the conductance of a wide range of molecules.[3] In contrast with other approaches, MCBJ is particularly impressive due to its compatibility with Si-based microfabrication and industrialisation. Recently, we have combined electrochemical deposition with MCBJ to develop an electrochemically assisted mechanically controllable break junction (EC-MCBJ) method[6] for characterizing molecular junctions conveniently and economically. Nevertheless, it is difficult to perform MCBJ for single-molecule conductance with a long molecular length due to the limited elastic deformation of the microchip. Here we successfully designed and synthesized three 1,3-butadiyne-linked binuclear ruthenium(II) organometallic wires by adapting the molecular lengths through modification of a chelating terpyridyl ligand so that the electrical conductance of these metal-inserted molecules could be investigated using our home-made EC-MCBJ method.

Compared with purely π-conjugated organic wire-like molecular systems such as oligoyne,[7] oligo(phenylene-ethynylene) (OPE),[8] oligo(phenylene-vinylene) (OPV),[9] and oligo(phenylene-imine) (OPI),[10] redox-active molecules are more promising as their conductance can be reversibly tuned with a gate electrode.[11] Moreover, electrochemical and spectroscopic studies[12] indicate that these redox-active conjugated molecular wires coupled with redox metal centres usually exhibit a much weaker dependence of the charge transport on molecular length, implying a better degree of electronic delocalization along the molecular backbones.

We have been interested in organometallic wires coupled with multiple redox-active metal centres linked by unsaturated carbon chains with extended π-conjugation.[13] A series of dinuclear ruthenium polyynediyl complexes capped with redox-active organometallic fragments $[(bph)(PPh_3)_2Ru]^+$ (bph = *N*-(benzoyl)-*N*′-(picolinylidene)-hydrazine)[13c] or $[(Phtpy)(PPh_3)_2Ru]^{2+}$ (Phtpy = 4′-phenyl-2,2′:6′,2″-terpyridine),[13b,c] were thus investigated. Intramolecular electron transfer is fine-tuned by

[a]*State Key Laboratory of Structural Chemistry, Fujian Institute of Research on the Structure of Matter, Chinese Academy of Sciences, Fuzhou, Fujian 350002, China. E-mail: czn@fjirsm.ac.cn*

[b]*State Key Laboratory of Physical Chemistry of Solid Surfaces and Department of Chemistry, College of Chemistry and Chemical Engineering, Xiamen University, Xiamen, Fujian 361005, China. E-mail: zqtian@xmu.edu.cn*

[c]*Zhejiang Key Laboratory for Reactive Chemistry on Solid Surfaces, Institute of Physical Chemistry, Zhejiang Normal University, Jinhua, Zhejiang 321004, China*

† Electronic supplementary information (ESI) available: Experimental details regarding synthesis and characterization, and figures giving additional spectral, electrochemical, molecular conductance measurement and DFT computational data. See DOI: 10.1039/c3sc50312g

‡ Hui-Min Wen and Yang Yang contributed equally.

successive insertion of 2,5-thiophene or 1,4-phenylene spacers to the bridging diacetylide as well as introducing electron-donating or electron-withdrawing substituents to the ancillary chelating ligands. The low HOMO–LUMO gaps ($E_g \approx 1.7$ eV)[13b] together with accessible functionalization[14] on these 1,3-butadiyne-linked dinuclear ruthenium(II) complexes prompt us to investigate their electrical conductance at the single-molecule level for the first time. Remarkably, these diruthenium(II) incorporated systems exhibit higher molecular conductance and weaker length dependence compared with OPE or OPV having comparable molecular lengths. This suggests that implanting redox-active ruthenium(II) centres into π-conjugated organic molecules is a feasible approach to access long molecular wires, which is significant to molecular electronics.

Results and discussion

The synthetic procedures and detailed characterization of TMSE- (TMSE = 2-(trimethylsilyl)ethyl) or acetyl-protected thiol-functionalized dinuclear ruthenium(II) complexes **1–3** (Scheme 1) are provided as ESI.†

Electrochemical studies on self-assembly monolayers (SAMs) based on acetyl-protective thiol-functionalized diruthenium complexes **1** and **2** on Au(111) electrodes were performed in a 0.1 M $NaClO_4$ aqueous solution. Two reversible redox waves (Fig. 1) were observed at 0.02 and 0.67 V (*vs.* SCE) with $\Delta E_{1/2}$ = 0.65 V due to stepwise one-electron processes $Ru_2^{II,II}/Ru_2^{III,II}$ and $Ru_2^{III,II}/Ru_2^{III,III}$, respectively. Obviously, the potential difference due to stepwise redox processes is more pronounced than that in solution ($\Delta E_{1/2}$ = 0.52 V), implying a larger redox coupling between two ruthenium centres in the SAMs. The redox potentials of SAMs based on **2** (Fig. S5†) are comparable to that of **1** except for a little anodic shift (~20 mV). A linear correlation of current intensity of the anodic and cathodic peaks with the scan rates demonstrated that both **1** and **2** were indeed self-assembled onto the surface of the gold electrode. The surface coverages[15] of **1** and **2** estimated from the charge of the anodic peak around 0.02 V are 4.1×10^{-11} and 3.7×10^{-11} mol cm^{-2}, respectively. They are comparable to the SAMs based on $[\{(AcS\text{-}CH_2C_6H_4tpy)(PPh_3)_2Ru\}_2\{\mu\text{-}N(CN)_2\}]^{3+}$ (4.0×10^{-11} mol cm^{-2})[14a] through single Au–S bonding, but are more than twice the experimental value of the SAMs based on a 1,3-butadiyne-bridged diruthenium(II) complex in a lying flat mode (1.5×10^{-11} mol cm^{-2}).[14b] In view of the calculated surface coverage, the molecular rigidity as well as the bulky auxiliary ligands such as PPh_3 and phenylterpyridyl, it is most likely that **1** and **2** are adsorbed onto the gold surface through Au–S bonding with single sulphur terminus. As a result, it is anticipated that Au–molecule–Au junctions could be formed when the complexes are assembled to adjustable nano-scale separations.

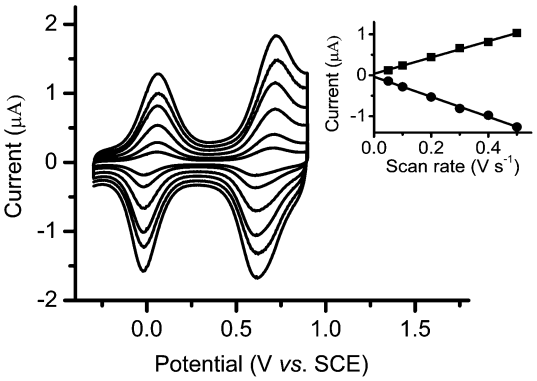

Fig. 1 Cyclic voltammograms (CVs) of self-assembly monolayers of complex **1** on Au(111) electrodes in 0.1 M $NaClO_4$ aqueous solution. The scan rates are 50, 100, 200, 300, 400, and 500 mV s^{-1}, respectively. Inset: linear dependence of the peak currents as a function of scan rates.

To investigate the single-molecule conductance of these thiol-functionalized dinuclear ruthenium(II) complexes, we used an EC-MCBJ approach under ambient conditions in our laboratory. Fig. 2a shows a schematic diagram of our home-made MCBJ compatible microchip after electrodeposition, of

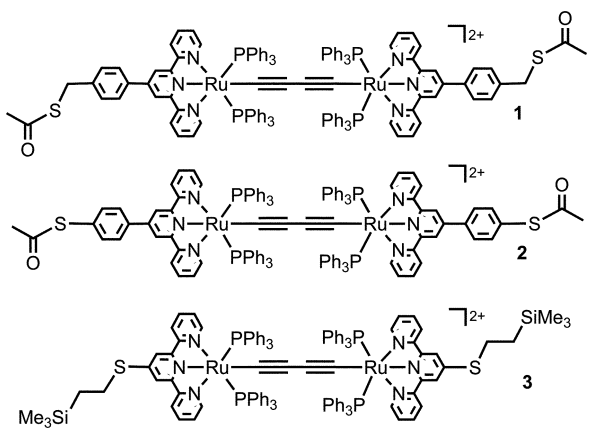

Scheme 1 Sulphur-functionalized dinuclear ruthenium(II) complexes **1–3**.

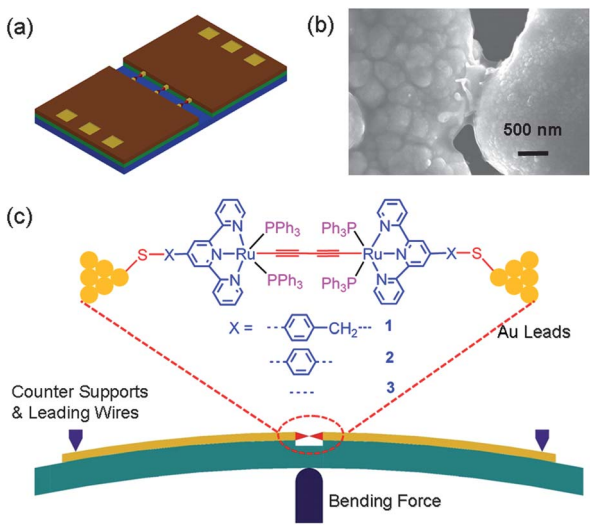

Fig. 2 (a) Schematic diagram of our microchip after electrodeposition. (b) Scanning electron microscopy (SEM) image of a typical Au electrode pair within the access window. (c) Au–molecule–Au junction constructed with a three-point bending mechanism.

which a detailed fabrication process can be found elsewhere.[6] Within the access window, Au atoms were deposited onto the exposed area to form a homogenous and compact layer over the original electrode pair. A typical scanning electron microscope (SEM) image of the access window part of the chip is given in Fig. 2b. The contact region of our electrode pair is around several hundred nanometers and the resistance is 100–200 Ω. The schematic diagram of our homemade EC-MCBJ device with a three-point bending mechanism is shown in Fig. 2c. The conductance of two model molecular junction systems including Au–BDT–Au (BDT = benzene-1,4-dithiol) and Au–BPY–Au (BPY = 4,4′-bipyridine) models[6b] had been tested successfully by our homemade EC-MCBJ device. Although the lengths of wire-like dinuclear ruthenium complexes are 2–3 times as long as BDT and BPY, our results show the feasibility of our economical EC-MCBJ method for statistical conductance analysis of these molecules. Details concerning the self-assembly processes and measurement procedures are given in the Experimental section (ESI†).

Each trial began with the characterization of the prepared Au electrode pairs without the measured molecule. Representative conductance curves during the breaking of electrode pairs and the corresponding histogram are given in Fig. S6 (ESI†). Just before the Au electrode pair breaks, stepwise conductance evolution and clear peaks for multiples of G_0 were observed in the conductance traces and histogram, respectively. In comparison, no plateaus and peaks can be found in the conductance traces and histogram below 1 G_0 value (Fig. S6†). The control experiments indicate that the peaks and corresponding conductance in the following experiments are attributed to the added target molecules.

Single-molecule conductance measurements of complexes **1–3** were carried out by bending and relaxing the microchips with a rate of 2 nm s^{-1}, and the bias applied to measure the conductance was 20 mV. For each molecule, about 400 conductance traces with discernible plateaus were collected in order to numerically generate the conductance histogram. Fig. 3 gives the representative conductance traces and related histograms. The peaks in histograms represent the most favourable conductance values in the recorded conductance traces for each complex, and are extensively counted as their single-molecule conductance values.[3a] As shown in Fig. 3, the histograms of **1**, **2**, and **3** display considerably distinct peaks at $3.0 \times 10^{-4}G_0$, $1.0 \times 10^{-3}G_0$, and $1.4 \times 10^{-3}G_0$, respectively, and no discernible lower peaks were observed in our experiments.

The high mechanical stability of our EC-MCBJ setup also offers the possibility for I–V_{bias} characterization. For each complex, the molecular junction was swept between −1.00 V and +1.00 V when the displacement of the stepping motor was frozen. Typical I–V_{bias} curves for molecules **1–3** are shown in Fig. S7 (ESI).† The I–V_{bias} curves are linear over a small bias range, from which the conductance is estimated as $3.5 \times 10^{-4}G_0$, $9.9 \times 10^{-4}G_0$, and $2.1 \times 10^{-3}G_0$, respectively, which are in good agreement with the values shown in the conductance histograms.

The conductance measurement results from both conductance histograms and I–V_{bias} characterizations suggest a sequence of **3** > **2** > **1** in single-molecule conductance, although they have comparable voltammetric behavior in solution and surface electrochemistry. The obvious conductance differences between them can be ascribed to the structural discrepancies in the auxiliary terpyridyl ligands of these dinuclear ruthenium complexes. Single-molecule conductance of **2** is about three times as large as that of **1**, implying that the methylene (–CH_2–) at each terminus of molecule **1** significantly prohibits charge transport along the molecular backbones. This result is well in accordance with that of thiol-terminated oligo(phenylenevinylene)s (OPVs).[9,16] Kushmerick *et al.* demonstrated that methylene groups at each end of OPVs would break the π-conjugated system and reduce molecular conductance to 5.4 nS, which is about one-third of the original value at 15.8 nS.[16] With a conversion based on 1 $G_0 \approx 77.6$ μS, 5.4 nS and 15.8 nS correspond to $7.0 \times 10^{-5}G_0$ and $2.0 \times 10^{-4}G_0$, respectively. This

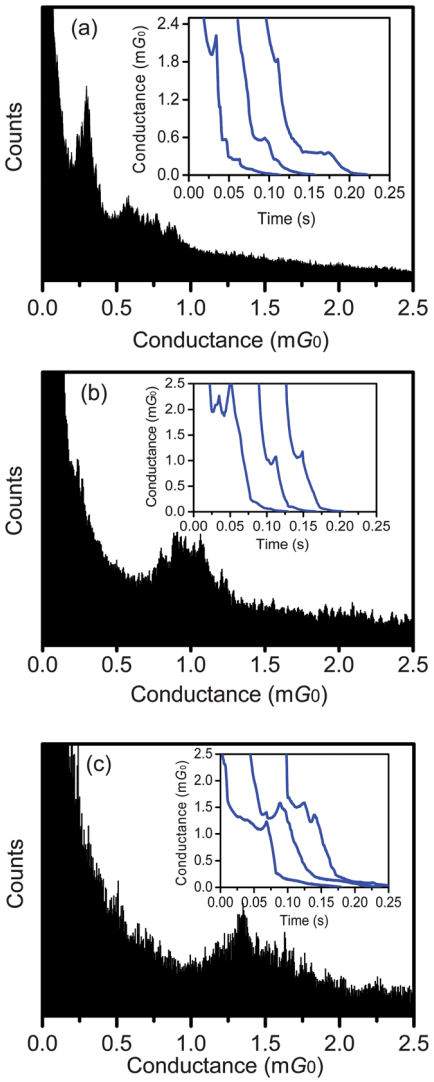

Fig. 3 Conductance histograms of dinuclear ruthenium(II) complexes (a) **1**, (b) **2**, and (c) **3** from hundreds of curves recorded in the MCBJ setup. Inset: typical conductance traces of the corresponding complexes **1**, **2**, and **3**, respectively. In the absence of dinuclear ruthenium(II) molecules, such steps and peaks are unobserved within the same conductance range.

implies that with removal of the methylene (–CH_2–) at each terminus of oligo(phenylenevinylene)s (OPVs),[9,16] the molecular conductance exhibits about three times enhancement (from $7.0 \times 10^{-5} G_0$ to $2.0 \times 10^{-4} G_0$). Thus, the increased magnitude of molecular conductance in diruthenium(II) implanted molecule **2** relative to **1** by removal of methylene (–CH_2–) at each terminus is comparable to that found in OPVs. More importantly, the measured results show that the single-molecular conductance of diruthenium(II) complex **2** ($1.0 \times 10^{-3} G_0$) is 5-fold as large as that of the π-conjugated OPV molecule ($2.0 \times 10^{-4} G_0$)[16] with a comparable length (*ca.* 2.9 nm), implying that **2** is much more conductive than the corresponding π-conjugated OPV molecule.

Compared with **2** (2.96 nm),[17] the intramolecular S···S distance was further reduced in **3** (2.09 nm) by removal of an aromatic ring (1,4-phenylene) at each terminal of **2**. The single-molecule conductance is slightly increased from $1.0 \times 10^{-3} G_0$ (**2**) to $1.4 \times 10^{-3} G_0$ (**3**), although there is a relatively large shortening in the molecular length of **3** compared with that of **2** (ΔL_m = 0.87 nm). It is known that in some well-studied π-conjugated organic molecular systems such as oligo(1,4-phenylene ethynylenes) (OPEs),[18] single-molecule conductance is usually increased by an order of magnitude when there is the same 0.87 nm decrease in molecular length. Compared with OPEs, the measured results suggest a smaller length dependence of conductivity for our molecules and thus a lower decay parameter for 1,3-butadiyene-linked diruthenium(II) complexes than that for OPEs. This is likely relevant to the much smaller HOMO–LUMO gap (*ca.* $E_g \approx 1.7$ eV) in **1–3** than the corresponding E_g values (3.3–3.6 eV) of OPE molecules.[8,18]

Remarkably, dinuclear ruthenium(II) complexes **1–3** showed a much better electrical conductance than the well-studied π-conjugated organic molecular wires with comparable molecular lengths. Single-molecule conductance of **3** ($1.4 \times 10^{-3} G_0$) is an order of magnitude larger than that of OPE (1,4-(4-$AcSC_6H_4C{\equiv}C)_2C_6H_4$, $0.96 \times 10^{-4} G_0$) measured using MCBJ devices under the same experimental conditions (Fig. S8†). With a conversion based on 1 $G_0 \approx 77.6$ μS, this measured value is equal to 7.4 nS. This measured value for OPE (7.4 nS) is comparable with those reported previously by Huber *et al.*,[8a] Wu *et al.*,[8b] and Kaliginedi *et al.*[18] (~9 nS) based on MCBJ measurements. Considering that the molecular length (2.01 nm) of OPE is comparable to **3** (2.09 nm), it is most likely that two ruthenium redox units, which are implanted into π-conjugated organic molecular backbones to form diruthenium complex **3**, exert positive effects on single-molecule conductance. Although it has been reported that the 2- to 3-fold higher molecular conductance for *trans*-$Pt(PR_3)_2(C{\equiv}CC_6H_4SAc)_2$ (R = Cy, Bu, Ph, OEt, OPh) than that for OPE (1,4-(4-$AcSC_6H_4C{\equiv}C)_2C_6H_4$) is due to a 1.6 Å decrease in sulphur-to-sulphur distance (1.85 nm as compared to 2.01 nm),[19] the 5-fold enhanced conductance in *trans*-$Ru(PPh_2CH_2PPh_2)_2(C{\equiv}CC_6H_4SAc)_2$ is undoubtedly ascribable to the structure of the Ru(II)-implanted backbone.[20] Our results further indicate that incorporating two redox-active ruthenium centres into π-conjugated organic molecular backbones is a potential approach for constructing long molecular wires with higher conductance and weaker length dependence than OPE or OPV having comparable length.

It has been suggested that aromatic 1,4-diacetylene derivatives usually follow a direct tunneling mechanism when the molecular lengths are within 4.4 nm.[12c] The molecular lengths of dinuclear ruthenium(II) complexes **1–3** (2–3 nm) fall within the range, in which direct tunnelling is likely the principal charge-transport mechanism. It is generally accepted that charge transport in aromatic thiol systems is a HOMO-mediated hole tunneling process.[8e,20] To address this issue, the molecular orbital energies of redox-active diruthenium complexes were estimated using the CV technique.[21] The relative positions of E_{HOMO} and E_{LUMO} states of **3** are shown in Fig. 4, along with the Fermi levels of the corresponding electrodes. Since the HOMO orbital is very close to the Fermi level of gold electrodes in energy, this leads most likely to a relatively lower length-dependent decay and higher conductance for **1–3**.

To compare the conductance characteristics of dinuclear Ru(II)-implanted complexes with π-conjugated organic molecules, we have calculated the electronic structures and transmission spectra at equilibrium state of these thiolate capped molecules connected to two semi-infinite gold electrodes. First, we optimized the geometry of the thiol capped molecules using DFT calculation.[17] The sulphur-to-sulphur distances were rather comparable for dinuclear Ru(II)-implanted complex **3** (2.09 nm), $HSC_6H_4C{\equiv}CC_6H_4C{\equiv}CC_6H_4SH$ (OPE3, 2.01 nm), and $HSC_6H_4C{\equiv}CC{\equiv}CC{\equiv}CC{\equiv}CC_6H_4SH$ (DPA4, 2.09 nm) (Fig. S9† and Table 1). The three optimized molecules were then positioned to the *z* direction in the hollow sites of both Au(111) electrode surfaces symmetrically at a favourable Au–S bonding distance (Fig. S10† for **3**).[8,22] The transmission spectra (Fig. 5) of the three extended molecular systems were finally calculated using an equilibrium Green functions technique based on DFT, as implemented in the TRANSIESTA package.[23,24]

The calculated conductance (Table 1) at zero-bias voltage was obtained according to the Landauer formula.[24,25] As depicted in

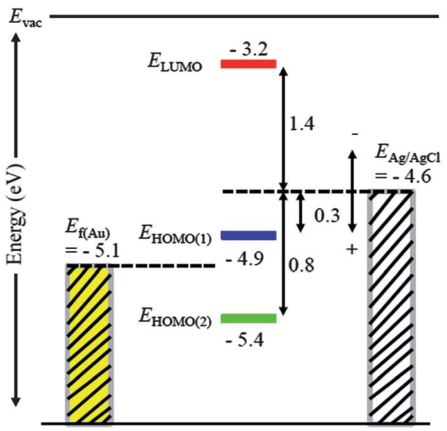

Fig. 4 Molecular orbital energy levels (HOMO and LUMO) of **3** as inferred from CV measurements in CH_2Cl_2 solution. The equivalent electrode work functions in the respective experimental setups have also been shown for comparison ($E_{f(Au)}$ = −5.1 eV, and $E_{f(Ag/AgCl)}$ = −4.6 eV). The molecular orbital energies (E_{HOMO} and E_{LUMO}) were estimated from the oxidation and reduction peaks (Fig. S4†) from CV measurements.

Table 1 The intramolecular S···S distance and zero-bias conductance $G(\mu, 0)$ of dinuclear Ru(II)-implanted complex **3** compared with organic molecules with similar length

	OPE3	DPA4	3
D_{S-S} (nm)	2.01	2.09	2.09
$G(\mu, 0)$ (G_0)	0.010	0.11	0.34

Fig. 5, the calculated transmission spectra indicate that complex **3** has a higher conductance than the corresponding π-conjugated organic molecules OPE3 and DPA4. The theoretical conductance of **3** is *ca.* 30-fold higher than that of OPE3, which is consistent with the fact that the measured conductance of **3** is as large as one order of magnitude over OPE3. Moreover, the 3-fold higher molecular conductance for **3** than that for DPA4 further suggests that incorporating two redox-active ruthenium centres into π-conjugated organic molecular backbones is indeed useful for constructing long molecular wires with higher conductance.

The calculated HOMO–LUMO gap of **3** (0.71 eV) is much smaller than that of OPE3 (2.42 eV) or DPA4 (1.62 eV). Although the calculated LUMO energy level of **3** is closer to the Fermi level of the gold electrode than the HOMO (Fig. S11†), the HOMO and LUMO related resonances overlap strongly to give a broad transmission band at zero-bias state as shown in Fig. 5. To confirm the conductance mechanism of dinuclear ruthenium molecules, we have projected the self-consistent Hamiltonian onto the HOMO and LUMO, respectively.[24,26] The MPSH (molecular projected self-consistent Hamiltonian) studies indicate that the HOMO of **3** (Fig. S12†) is mainly resident on the Ru–C≡C–C≡C–Ru backbone of the molecule, composed of dπ(Ru) and π(C≡C–C≡C) orbitals, which is consistent with the direction of electron transport. On the contrary, the LUMO is primarily distributed on π orbitals of the ancillary terpyridyl ligands on each side of the molecule, in which the electronic density is scarcely resident on the Ru–C≡C–C≡C–Ru backbone, which is unfavourable for electron transport. Thus, the HOMO-mediated electron transport process suggested by the theoretical calculation is in agreement with the result of CV studies.

Based on the HOMO-mediated hole tunneling mechanism, it is readily understandable that the molecular conductance difference between **2** and **3** is small in view of only a minor contribution from the ancillary terpyridyl ligand to the HOMO. In contrast, it is likely to modulate the molecular conductance in a more remarkable degree by substitution of 1,3-butadiyene with the more extended aromatic diacetylene system because electronic communication between two redox-active ruthenium centres could be significantly modified by changing the lengths of π-conjugated linkers,[13] which is the focus of the next-step of studies.

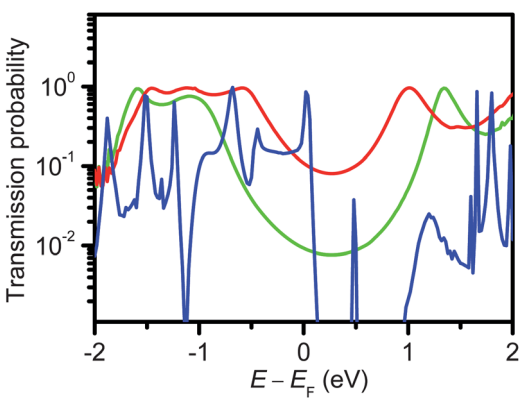

Fig. 5 Transmission spectra at equilibrium state (in log scale) of **3** (blue), OPE3 (green), and DPA4 (red) around the Fermi level of the electrodes which are set to zero for convenience.

Conclusions

Single-molecule conductance of diruthenium(II) coordinated molecules containing two Ru(II) redox centres linked by 1,3-butadiyne was investigated for the first time in our homemade MCBJ setup. The molecular lengths of 1,3-butadiyne-linked dinuclear ruthenium complexes were designed to an applicable value and the anchoring groups were tailored on thiol-functionalized chelating tripyridyl ligands, making MCBJ characterization for dinuclear ruthenium(II) complexes feasible. It is demonstrated that dinuclear ruthenium(II) complexes exhibit higher molecular conductance and weaker length dependence than that of OPE or OPV with comparable length. Modulation of molecular conductance is achieved by changing the length and π-conjugated system of the chelating tripyridyl ligands. It was verified that the capability of our time-effective and cost-effective EC-MCBJ method can be extended to the molecules with a length of 2–3 nm. Moreover, surface electrochemistry demonstrated that there were multi-redox-active centres for 1,3-butadiyne-bridged dinuclear ruthenium complexes, especially in the region of electrochemical windows, which gives the potential to achieve electrochemical gating of molecular conductance. This may open the door to constitute multi-switched states of active molecular devices in the future.

Acknowledgements

This work was supported by the NSFC (20931006, U0934003, and 91122006) and the NSF of Fujian Province (2011J01065). The authors thank Dr L.-H. Li (Northwestern Univ.) for the help regarding theoretical calculations of electronic transport. The authors also thank Dr S. Jin (Central China Normal Univ.) for providing the OPE sample.

Notes and references

1 A. Aviram and M. A. Ratner, *Chem. Phys. Lett.*, 1974, **29**, 277.
2 J. C. Cuevas and E. Scheer, *Molecular Electronics; An Introduction to Theory and Experiment*, World Scientific, Singapore, 2010.
3 (*a*) B. Xu and N. J. Tao, *Science*, 2003, **301**, 1221; (*b*) H. Song, M. A. Reed and T. Lee, *Adv. Mater.*, 2011, **23**, 1583; (*c*) R. L. McCreery, *Chem. Rev.*, 2008, **108**, 2646; (*d*) B. Ulgut

and H. D. Abruna, *Chem. Rev.*, 2008, **108**, 2721; (*e*) L. Venkataraman, J. E. Klare, C. Nuckolls, M. S. Hybertsen and M. L. Steigerwald, *Nature*, 2006, **442**, 904; (*f*) J. G. Kushmerick, D. B. Holt, S. K. Pollack, M. A. Ratner, J. C. Yang, T. L. Schull, J. Naciri, M. H. Moore and R. Shashidhar, *J. Am. Chem. Soc.*, 2002, **124**, 10654; (*g*) N. Agraït, A. L. Yeyati and J. M. van Ruitenbeek, *Phys. Rep.*, 2003, **377**, 81.

4 (*a*) Y. Ie, T. Hirose, H. Nakamura, M. Kiguchi, N. Takagi, M. Kawai and Y. Aso, *J. Am. Chem. Soc.*, 2011, **133**, 3014; (*b*) Y. Ie, M. Endou, S. K. Lee, R. Yamada, H. Tada and H. Aso, *Angew. Chem., Int. Ed.*, 2011, **50**, 11980; (*c*) F. B. Meng, Y.-M. Hervault, L. Norel, K. Costuas, C. Van Dyck, V. Geskin, J. Cornil, H. H. Hng, S. Rigaut and X. D. Chen, *Chem. Sci.*, 2012, **3**, 3113.

5 (*a*) T. Kurita, Y. Nishimori, F. Toshimitsu, S. Muratsugu, S. Kume and H. Nishihara, *J. Am. Chem. Soc.*, 2010, **132**, 4524; (*b*) I.-W. P. Chen, M.-D. Fu, W.-H. Tseng, J.-Y. Yu, S.-H. Wu, C.-J. Ku, C. H. Chen and S.-M. Peng, *Angew. Chem., Int. Ed.*, 2006, **45**, 5814; (*c*) C. X. Yin, G.-C. Huang, C.-K. Kuo, M.-D. Fu, H.-C. Lu, J.-H. Ke, K.-N. Shih, Y.-L. Huang, G.-H. Lee, C.-Y. Yeh, C.-H. Chen and S.-M. Peng, *J. Am. Chem. Soc.*, 2008, **130**, 10090; (*d*) N. Tuccitto, V. Ferri, M. Cavazzini, S. Quici, G. Zhavnerko, A. Licciardello and M. A. Rampi, *Nat. Mater.*, 2009, **8**, 41.

6 (*a*) Y. Yang, J.-Y. Liu, Z.-B. Chen, J.-H. Tian, X. Jin, B. Liu, X. Li, Z.-Z. Luo, M. Lu, F.-Z. Yang, N. Tao and Z.-Q. Tian, *Nanotechnology*, 2011, **22**, 275313; (*b*) Y. Yang, Z. Chen, J. Liu, M. Lu, D. Yang, F. Yang and Z. Tian, *Nano Res.*, 2011, **4**, 1199.

7 (*a*) C. Wang, A. S. Batsanov, M. R. Bryce, S. Martin, R. J. Nichols, S. J. Higgins, V. M. Garcia-Suarez and C. J. Lambert, *J. Am. Chem. Soc.*, 2009, **131**, 15647; (*b*) V. M. Garcia-Suarez and C. J. Lambert, *Nanotechnology*, 2008, **19**, 455203.

8 (*a*) R. Huber, M. T. González, S. Wu, M. Langer, S. Grunder, V. Horhoiu, M. Mayor, M. R. Bryce, C. Wang, R. Jitchati, C. Schönenberger and M. Calame, *J. Am. Chem. Soc.*, 2008, **130**, 1080; (*b*) S. Wu, M. T. González, R. Huber, S. Grunder, M. Mayor, C. Schönenberger and M. Calame, *Nat. Nanotechnol.*, 2008, **3**, 569; (*c*) Q. Lu, K. Liu, H. Zhang, Z. Du, X. Wang and F. Wang, *ACS Nano*, 2009, **3**, 3861; (*d*) W. Hong, D. Z. Manrique, P. Moreno-García, M. Gulcur, A. Mishchenko, C. J. Lambert, M. R. Bryce and T. Wandlowski, *J. Am. Chem. Soc.*, 2012, **134**, 2292; (*e*) S. Martin, I. Grace, M. R. Bryce, C. Wang, R. Jitchati, A. S. Batsanov, S. J. Higgins, C. J. Lambert and R. J. Nichols, *J. Am. Chem. Soc.*, 2010, **132**, 9157; (*f*) K. Liu, G. Li, X. Wang and F. Wang, *J. Phys. Chem. C*, 2008, **112**, 4342.

9 A. Danilov, S. Kubatkin, S. Kafanov, P. Hedegård, N. Stuhr-Hansen, K. Moth-Poulsen and T. Bjørnholm, *Nano Lett.*, 2008, **8**, 1.

10 (*a*) S. H. Choi, B. Kim and C. D. Frisbie, *Science*, 2008, **320**, 1482; (*b*) S. H. Choi, C. Risko, M. C. R. Delgado, B. Kim, J.-L. Brédas and C. D. Frisbie, *J. Am. Chem. Soc.*, 2010, **132**, 4358.

11 (*a*) W. Haiss, R. J. Nichols, S. J. Higgins, D. Bethell, H. Höbenreich and D. J. Schiffrin, *Faraday Discuss.*, 2004, **125**, 179; (*b*) N. Darwish, I. Díez-Pérez, P. Da Silva, N. Tao, J. J. Gooding and M. N. Paddon-Row, *Angew. Chem., Int. Ed.*, 2012, **51**, 3203; (*c*) K. Seo, A. V. Konchenko, J. Lee, G. S. Bang and H. Lee, *J. Am. Chem. Soc.*, 2008, **130**, 2553; (*d*) X.-S. Zhou, L. Liu, P. Fortgang, A.-S. Lefevre, A. Serra-Muns, N. Raouafi, C. Amatore, B.-W. Mao, E. Maisonhaute and B. Schöllhorn, *J. Am. Chem. Soc.*, 2011, **133**, 7509.

12 (*a*) A. S. Blum, T. Ren, D. A. Parish, S. A. Trammell, M. H. Moore, J. G. Kushmerick, G.-L. Xu, J. R. Deschamps, S. K. Pollack and R. Shashidhar, *J. Am. Chem. Soc.*, 2005, **127**, 10010; (*b*) L. Luo, A. Benameur, P. Brignou, S. H. Choi, S. Rigaut and C. D. Frisbie, *J. Phys. Chem. C*, 2011, **115**, 19955; (*c*) B. Kim, J. M. Beebe, C. Olivier, S. Rigaut, D. Touchard, J. G. Kushmerick, X.-Y. Zhu and C. D. Frisbie, *J. Phys. Chem. C*, 2007, **111**, 7521; (*d*) T. Ren, *Organometallics*, 2005, **24**, 4854; (*e*) G.-L. Xu, G. Zou, Y.-H. Ni, M. C. DeRosa, R. J. Crutchley and T. Ren, *J. Am. Chem. Soc.*, 2003, **125**, 10057; (*f*) M. A. Fox, R. L. Roberts, T. E. Baines, B. Le Guennic, J.-F. Halet, F. Hartl, D. S. Yufit, D. Albesa-Jove, J. A. K. Howard and P. J. Low, *J. Am. Chem. Soc.*, 2008, **130**, 3566; (*g*) C. Olivier, K. Costuas, S. Choua, V. Maurel, P. Turek, J.-Y. Saillard, D. Touchard and S. Rigaut, *J. Am. Chem. Soc.*, 2010, **132**, 5638.

13 (*a*) L.-B. Gao, L.-Y. Zhang, L.-X. Shi and Z.-N. Chen, *Organometallics*, 2005, **24**, 1678; (*b*) L.-B. Gao, S.-H. Liu, L.-Y. Zhang, L.-X. Shi and Z.-N. Chen, *Organometallics*, 2006, **25**, 506; (*c*) L.-B. Gao, J. Kan, Y. Fan, L.-Y. Zhang, S.-H. Liu and Z.-N. Chen, *Inorg. Chem.*, 2007, **46**, 5651.

14 (*a*) H.-M. Wen, D.-B. Zhang, L.-Y. Zhang, L.-X. Shi and Z.-N. Chen, *Eur. J. Inorg. Chem.*, 2011, **11**, 1784; (*b*) L.-Y. Zhang, H.-X. Zhang, S. Ye, H.-M. Wen, Z.-N. Chen, M. Osawa, K. Uosaki and Y. Sasaki, *Chem. Commun.*, 2011, **47**, 923.

15 A surface coverage Γ of self-assembly films was determined according to equation $\Gamma = Q/nFA$, where Q, n, F, and A are the charge required to oxidize the ruthenium centers determined from the area under the anodic peak around 0.02 V of **1** and **2**, the number of electrons transferred ($n = 1$), the Faraday's constant, and the area of electrodes.

16 D. S. Seferos, A. S. Blum, J. G. Kushmerick and G. C. Bazan, *J. Am. Chem. Soc.*, 2006, **128**, 11260.

17 The optimized geometrical structures of thiol capped molecules were performed by density functional theory (DFT) approximation at the B3PWP91/6-311G**/Lanl2dz(f) level.

18 V. Kaliginedi, P. Moreno-García, H. Valkenier, W. J. Hong, V. M. García-Suárez, P. Buiter, J. L. H. Otten, J. C. Hummelen, C. J. Lambert and T. Wandlowski, *J. Am. Chem. Soc.*, 2012, **134**, 5262.

19 (*a*) T. L. Schull, J. G. Kushmerick, C. H. Patterson, C. George, M. H. Moore, S. K. Pollack and R. Shashidhar, *J. Am. Chem. Soc.*, 2003, **125**, 3202; (*b*) M. Mayor, C. von Hänisch, H. B. Weber, J. Reichert and D. Beckmann, *Angew. Chem., Int. Ed.*, 2002, **41**, 1183.

20 K. Liu, X. Wang and F. Wang, *ACS Nano*, 2008, **2**, 2315.

21 (*a*) B. Q. Xu, X. L. Li, Y. Xiao, H. Sakaguchi and N. J. Tao, *Nano Lett.*, 2005, **5**, 1491; (*b*) A. K. Mahapatro, J. Ying, T. Ren and D. B. Janes, *Nano Lett.*, 2008, **8**, 2131.
22 Ž. Crljen and G. Baranović, *Phys. Rev. Lett.*, 2007, **98**, 116801.
23 J. M. Soler, E. Artacho, J. D. Gale, A. García, J. Junquera, P. Ordejón and D. Sanchez-Portal, *J. Phys.: Condens. Matter*, 2002, **14**, 2745.
24 M. Brandbyge, J.-L. Mozos, P. Ordejón, J. Taylor and K. Stokbro, *Phys. Rev. B: Condens. Matter Mater. Phys.*, 2002, **65**, 165401.
25 Y. Imry and R. Landauer, *Rev. Mod. Phys.*, 1999, **71**, S306.
26 J. Taylor, H. Guo and J. Wang, *Phys. Rev. B: Condens. Matter Mater. Phys.*, 2001, **63**, 245407.